Iowa State University

From the SelectedWorks of Scott Nelson

January, 2007

The T4 Phage UvsW Protein Contains Both DNA Unwinding and Strand Annealing Activities

Scott W. Nelson, *Pennsylvania State University - Main Campus*
Stephen J. Benkovic, *Pennsylvania State University - Main Campus*

Available at: https://works.bepress.com/scott-nelson/4/

THE JOURNAL OF BIOLOGICAL CHEMISTRY VOL. 282, NO. 1, pp. 407–416, January 5, 2007
© 2007 by The American Society for Biochemistry and Molecular Biology, Inc. Printed in the U.S.A.

The T4 Phage UvsW Protein Contains Both DNA Unwinding and Strand Annealing Activities*[S]

Received for publication, August 24, 2006, and in revised form, November 7, 2006 Published, JBC Papers in Press, November 8, 2006, DOI 10.1074/jbc.M608153200

Scott W. Nelson[1] **and Stephen J. Benkovic**[2]

From the Department of Chemistry, The Pennsylvania State University, University Park, Pennsylvania 16802

UvsW protein belongs to the SF2 helicase family and is one of three helicases found in T4 phage. UvsW governs the transition from origin-dependent to origin-independent replication through the dissociation of R-loops located at the T4 origins of replication. Additionally, *in vivo* evidence indicates that UvsW plays a role in recombination-dependent replication and/or DNA repair. Here, the biochemical properties of UvsW helicase are described. UvsW is a 3′ to 5′ helicase that unwinds a wide variety of substrates, including those resembling stalled replication forks and recombination intermediates. UvsW also contains a potent single-strand DNA annealing activity that is enhanced by ATP hydrolysis but does not require it. The annealing activity is inhibited by the non-hydrolysable ATP analog (adenosine 5′-*O*-(thiotriphosphate)), T4 single-stranded DNA-binding protein (gp32), or a small 8.8-kDa polypeptide (UvsW.1). Fluorescence resonance energy transfer experiments indicate that UvsW and UvsW.1 form a complex, suggesting that the UvsW helicase may exist as a heterodimer *in vivo*. Fusion of UvsW and UvsW.1 results in a 68-kDa protein having nearly identical properties as the UvsW-UvsW.1 complex, indicating that the binding locus of UvsW.1 is close to the C terminus of UvsW. The biochemical properties of UvsW are similar to the RecQ protein family and suggest that the annealing activity of these helicases may also be modulated by protein-protein interactions. The dual activities of UvsW are well suited for the DNA repair pathways described for leading strand lesion bypass and synthesis-dependent strand annealing.

With the exception of host cell RNA polymerase, bacteriophage T4 supplies all the proteins necessary for the replication and repair of its 169-kilobase linear genome (1). T4 phage encodes for three helicases: gp41,[3] Dda, and UvsW. Both gp41 and Dda helicase have been extensively characterized biochemically (2–5). On the other hand, very little is known about the biochemical properties of UvsW helicase. The majority of the functional information regarding UvsW comes from *in vivo* experiments studying the effects of UvsW loss-of-function mutants alone or in combination with other gene knockouts (6–8). Through these *in vivo* experiments, the Kreuzer laboratory (9) has demonstrated that UvsW regulates the initiation of DNA replication from T4 origins and plays a role in recombination and/or DNA repair.

T4 phage utilizes two methods for the initiation of its replication: origin-dependent, which requires *Escherichia coli* RNA polymerase to synthesize a stably bound R-loop, and origin-independent, which requires the T4 proteins UvsX and UvsY to catalyze recombination between single-stranded DNA (ssDNA) and homologous double-stranded DNA (dsDNA) (10). A controlling factor governing the transition between these two modes of initiation is the UvsW protein, which has been shown both *in vitro* and *in vivo* to dissociate R-loops from the origins of replication in T4 phage (11). Partially based on this ability, UvsW has been described as a functional analog of the *E. coli* RecG protein. In support of this, expression of UvsW is able to complement some of the defects in RecG$^-$ *E. coli* (9).

In comparison to what is known regarding the function of UvsW in the initiation of replication, the precise role of UvsW in recombination and DNA repair is much less clear. Inactivation of the UvsW gene results in sensitivity to hydroxyurea and UV light, indicating some role in the processing of damaged DNA and stalled replication forks (12–14). Additionally, the inactivation of the T4 Holliday junction endonuclease (gp49) does not completely eliminate the ability of T4 phage to resolve branched DNA structures, suggesting an alternative mechanism for resolution (15). The Kreuzer laboratory (9) has demonstrated the ability of UvsW to unwind a three-way branched DNA substrate, strongly suggesting that UvsW is responsible for branch migration in T4 phage. However, a complete description of the biochemical properties of UvsW is lacking, making the assignment of addition roles for UvsW in DNA repair difficult.

Even though there have been few *in vitro* studies of UvsW function, an x-ray crystal structure of a truncated UvsW mutant has been solved (Ref. 16; Fig. 1). The structure consists of one of the two predicted RecA-like domains and a putative substrate binding domain resembling a "double wing" motif (17). Based on this structure, a model for UvsW-catalyzed unwinding has been proposed that is consistent with previous descriptions of the "inchworm" model (18). This model relies on the two RecA-like domains to undergo alternating opening

* This work was supported by National Institutes of Health Grants GM13306 (to S. J. B.). The costs of publication of this article were defrayed in part by the payment of page charges. This article must therefore be hereby marked "*advertisement*" in accordance with 18 U.S.C. Section 1734 solely to indicate this fact.

[S] The on-line version of this article (available at http://www.jbc.org) contains supplemental Fig. 1.

[1] A Fellow of the Jane Coffin Childs Memorial Fund for Medical Research.

[2] To whom all correspondence should be addressed: Dept. of Chemistry, The Pennsylvania State University, University Park, PA 16802. Tel.: 814-865-2882; Fax: 814-865-2973; E-mail: sjb1@psu.edu.

[3] The abbreviations used are: gp, gene product; ssDNA, single-stranded DNA; dsDNA, double-stranded DNA; CPM, 7-diethylamino-3-(4′-maleimidylphenyl)-4-methylcoumarin; UvsW/W.1, an equimolar mixture of UvsW and UvsW.1 proteins; UvsW-W.1, a fusion of UvsW.1 to the C terminus of UvsW; ATPγS, adenosine 5′-*O*-(thiotriphosphate); CBD/intein, C-terminal chitin binding and intein domain; SDSA, synthesis-dependent strand annealing.

Downloaded from http://www.jbc.org/ at IOWA STATE UNIV on March 28, 2016

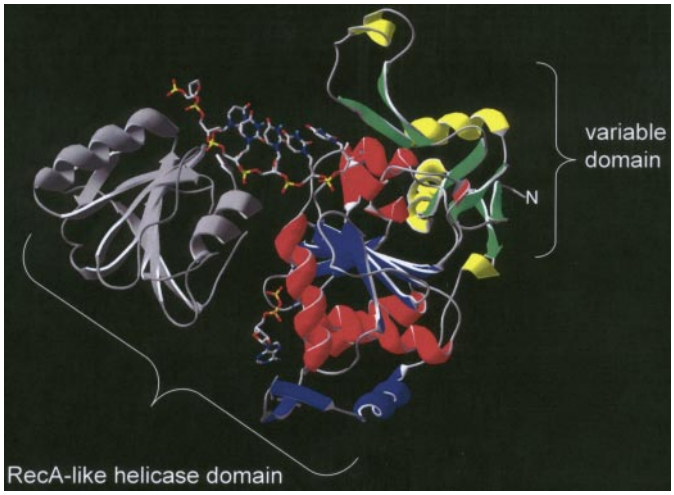

FIGURE 1. **Structural model of the UvsW protein.** The model was generated by alignment of the RecA-like helicase domains from UvsW, HCV NS3, and RecG proteins using the SuperPose V1.0 server with PDB codes 1RIF, 1A1V, 1GM5, respectively. Shown in *yellow* and *green* is the variable MotCF-like winged helix domain from UvsW. The RecA-like helicase domain from UvsW is shown in *red* and *blue*. The second RecA-like helicase domain colored in *gray* is from the HCV NS3 structure. The ssDNA bound to the helicase domains is from the HCV NS3 structure, and the ADP moiety bound at the interface between the helicase domains comes from the RecG structure.

and closing structural changes while translocating on DNA. The structure of UvsW revealed that there is very little structural homology shared between RecG and UvsW outside of the RecA-like domains, leading to the suggestion that UvsW and RecG recognize their nucleic acid substrates through different mechanisms (19, 16).

To complement the functional data from *in vivo* experiments and structural information from the x-ray crystallography, we have carried out biochemical experiments using purified full-length UvsW protein. We show that UvsW is a DNA-dependent ATPase that is capable of unwinding a variety of DNA/DNA and RNA/DNA substrates, with a preference for structures resembling stalled replication forks and recombination intermediates. Surprisingly, UvsW also possesses an ssDNA annealing activity that can be partially inhibited by ssDNA-binding protein (gp32) or a small 8.8-kDa polypeptide (UvsW.1). We demonstrate with fluorescence resonance energy transfer experiments that that UvsW and UvsW.1 form a complex and that fusion of UvsW.1 to the C terminus of UvsW reproduces the effects of UvsW.1 addition. Based on these properties, we suggest that the biochemical properties of UvsW are most similar to the RecQ protein family and that the annealing activity of these helicases may also be modulated by interaction with other proteins. Additionally, the dual activities of UvsW are well suited for several DNA repair pathways that require both unwinding and annealing activities.

MATERIALS AND METHODS

[γ-^{32}P]ATP was purchased from PerkinElmer Life Sciences. Unlabeled ribonucleotides were purchased from Roche Applied Science. 7-Diethylamino-3-(4′-maleimidylphenyl)-4-methylcoumarin (CPM) was obtained from Molecular Probes (Eugene, OR). Bacteriophage T4 gp32 were purified as described (20). The pGEM, pTYB3, and pet28a vectors were from Promega, New England Biolabs, and Novagen, respectively. T4 genomic DNA was obtained from Sigma. RecA protein and the chitin resin came from New England Biolabs.

Cloning, Expression, and Purification of UvsW Helicase—The open reading frame encoding UvsW helicase was PCR-amplified from T4 genomic DNA using the following forward and reverse primers, respectively: 5′-GCGGCAGCCATATGGATATTAAAGTACATTTTCACGAC-3′ and 5′-GTCGGATCCCGTAAATTAACTGTTTTCATTAC-3′. The underlined sequences indicate NdeI and BamHI restriction sites, respectively, which were used to clone the PCR product into the pet28a expression vector. The pet28a vector supplies a hexahistidine tag at the N terminus of the protein, which is connected to the open reading frame of UvsW by a 10-residue amino acid linker. The vector containing the gene for UvsW was transformed into BL21 (DE3) *E. coli*, and a single colony was used to inoculate a 20 ml of overnight culture of Luria broth. Two liters of Luria broth in two 2-liter flasks were inoculated with 10 ml of overnight culture each and grown to an absorbance of 1.0 at 600 nm. The cells were then cooled to 18 °C, induced with 0.15 mM isopropyl 1-thio-β-D-galactopyranoside, and allowed to grow an additional 16 h before being harvested by centrifugation at 6000 × *g*. The harvested cell pellet was resuspended in 60 ml of 20 mM Tris-HCl, 500 mM NaCl, and 5 mM imidazole (pH 8.0) and lysed using sonication. After centrifugation at 17,000 × *g* for 45 min, the cell-free extract was loaded onto a nickel nitrilotriacetic acid-agarose column and washed with 50 of lysis buffer containing 40 mM imidazole followed by 50 column volumes of lysis buffer containing 40 mM imidazole and 1 M NaCl. Lysis buffer containing 100 mM imidazole eluted UvsW from the column. The eluted protein was diluted 3-fold with P11-A buffer (20 mM Tris-HCl, 400 mM NaCl (pH 7.5)) and loaded onto a 20-ml P11 phosphocellulose column that was pre-equilibrated in P11-A. The column was washed with 10 column volumes of the same buffer before eluting UvsW with a 0.4–1.5 M NaCl gradient. UvsW eluted at a NaCl concentration of ~1 M. UvsW was concentrated to 10 μM using an Amicon centrifugation device and frozen in aliquots at −80 °C. Protein concentration was calculated based on an extinction coefficient of 73920 M^{-1} cm^{-1}.

Cloning, Expression, and Purification of UvsW.1 and UvsW/W.1 Fusion Proteins—The UvsW operon was PCR-amplified from T4 genomic DNA using the following forward and reverse primers, respectively: 5′-GATCGATACCATGGTACTAGAATTTAAACAATTTC-3′ and 5′-GGTGGTTGCTCTTCCAACAAAGCTTTCTTCTACTTC-3′. The underlined sequences indicate NcoI and SapI restriction sites, respectively, which were used to clone the PCR product into the pTYB3 expression vector. The pTYB3 vector aids in the purification of the 8.8-kDa peptide via an intein/chitin binding domain fused to the C terminus. UvsW.1 was expressed in Bl21 (DE3) cells in an identical fashion as UvsW. The harvested cell pellet was resuspended in 60 ml of 20 mM Tris acetate, 500 mM sodium acetate, and 1 mM EDTA (pH 7.8) and lysed using sonication. After centrifugation at 17,000 ×

Downloaded from http://www.jbc.org/ at IOWA STATE UNIV on March 28, 2016

g for 45 min, the cell-free extract was loaded onto a 5-ml chitin column and washed overnight with 2 liters of 20 mM Tris acetate, 1 M NaCl, 1 mM EDTA (pH 7.8). After the wash, the column was resuspended in 20 ml of lysis buffer containing 75 mM β-mercaptoethanol and incubated at 4 °C for 24 h to facilitate intein mediated cleavage. After cleavage, UvsW.1 was eluted from the column using lysis buffer and dialyzed into 10 mM Tris acetate, 50 mM potassium acetate, 5 mM magnesium acetate, and 20% glycerol (pH 7.8). Protein concentration was calculated based on an extinction coefficient of 3900 M^{-1} cm^{-1}. The UvsW/W.1 fusion was constructed by performing QuikChange™ site-directed mutagenesis on the pTYB3-UvsW operon vector using the following forward primer (reverse primer is the reverse-complement of forward): 5′-CGT AAT GAA AAC AGT TAA TTT AAT AAG CTT CGG CCC TTT GGA G-3′. The mutation was confirmed using dideoxy sequencing. The fusion protein was purified essentially as described for UvsW.1 with an additional phosphocellulose column (P11) carried out in an identical fashion as that of UvsW. Protein concentration was determined using the same extinction coefficient as UvsW.

Labeling of UvsW.1 with 7-Diethylamino-3-(4′-maleimidylphenyl)-4-methylcoumarin—UvsW.1 was extensively dialyzed into labeling buffer (20 mM Hepes, 100 mM NaCl (pH 7.0), and diluted to a concentration of 20 μM before labeling with a 20-fold excess of CPM for 2 h at room temperature. The reaction (1 ml) was quenched with 2 mM β-mercaptoethanol and dialyzed against four 1-liter changes of labeling buffer. Labeling efficiency was ~95%, as determined by the protein/label ratio.

DNA Constructs—Oligonucleotide substrate specificity studies were performed using various combinations of the following primers: P1, 5′-CATCATGCAGGACAGTCGGATCGGAGTCAGATTTACTGTGTCATATAGTACGTATTCAGT-3′; P2, 5′-TAACGTATTCAAGATACCTCGTACTCTGTACTGACTCCGATCCGACTGTCCTGCATGATG-3′; P3, 5′-ACTGAATACGTACTATATGACACAGTAAA-3′; P4, 5′-ACAGAGTACGAGGTATCTTGAATACGTTA-3′. The combination of oligonucleotides annealed to make the DNA substrates can be found in Table 1. All substrates were annealed before 5′ phosphorylation with [γ-^{32}P]ATP (8000 mCi/mmol, PerkinElmer Life Sciences) using polynucleotide kinase under standard conditions.

The R-loop substrate (pGEM-ori) was synthesized using a supercoiled 3.53-kilobase pGEM vector containing the T4 DNA replication origin oriF (positions 114754–115284 of the T4 genome). 10 μg of the vector was treated with 50 units of T7 RNA polymerase in the presence of 0.2 mM ribonucleotide triphosphates and 10 μCi of [α-^{32}P]CTP (3000 mCi/mmol) at 37 °C for 30 min. The reaction was purified using Qiagen spin columns following the manufacturer's instructions. The concentration and purity of the R-loop-containing vector was determined using a 1% agarose gel using 0.5× Tris borate EDTA as a buffer.

The D-loop substrate was synthesized as described with minor modifications (21). The invading oligonucleotide (300 nM), with a sequence of 5′-CGCGAATTTTAACAAAATATTAACGCTTACAATTTCCTGATGCGGTATTTTCTCCTTACGCATCTGTGCGGTATTTCAC-3′, was polynucleotide kinase-labeled with [γ-^{32}P]ATP. The oligonucleotide was diluted 10-fold and incubated in replication buffer (25 mM Tris acetate (pH 7.8), 125 mM potassium acetate, and 10 mM magnesium acetate) with 0.75 μM RecA protein for 5 min at 37 °C in the presence of 2 mM ATP, 20 mM creatine phosphate, and 2 units/ml of creatine kinase. After the preincubation period, the pGEM-ori vector was added to a concentration of 70 nM to initiate the strand invasion reaction. The reaction was allowed to proceed for 1.45 min before the addition of helicase.

TABLE 1

Structures of oligonucleotide-based substrates used for DNA unwinding and strand annealing reactions

oligonucleotides	DNA structure
P1 + P3	A
P2 + P4	B
P1 + P2	C
P1 + P2+ P3	D
P1 + P2 + P4	E
P1 + P2 + P3 + P4	F

Nucleotide Hydrolysis Assays—Hydrolysis of triphosphate nucleotides (ATP, GTP, dATP, CTP, UTP) was monitored at 340 nm using pyruvate kinase and lactate dehydrogenase to couple the phosphorylation of nucleoside diphosphates by phosphoenolpyruvate to the oxidation of NADH to NAD^+. The reactions were performed at 25 °C in complex buffer containing 0.2 mM NADH, 2 mM phosphoenolpyruvate, 10 units of pyruvate kinase, and 5 units of lactate dehydrogenase. For nucleotide specificity, K_mATP, and k_{cat} determination, the concentration of UvsW and ssDNA M13 were 20 nM and 2 μM, respectively. Substrate specificity assays used a duplex made up of oligonucleotides P1 and P3 (substrate A in Table 1), a duplex using P4 and the complement to P4, and ssDNAs P1 and P3. The validity of the coupled assay was confirmed by a linear relationship, starting at the origin, in plots of velocity *versus* UvsW concentration. Initial rate data were fitted to the Michaelis-Menten equation using IgorPro software.

Fluorescence Experiments—All steady-state fluorescence experiments were carried out on an ISA FluoroMax-2 spectrofluorometer at 25 °C using slit widths of 2 nm for both excitation and emission. UvsW.1-CPM (200 nM) was mixed with UvsW (200 nM) in replication buffer. An excitation wavelength

Downloaded from http://www.jbc.org/ at IOWA STATE UNIV on March 28, 2016

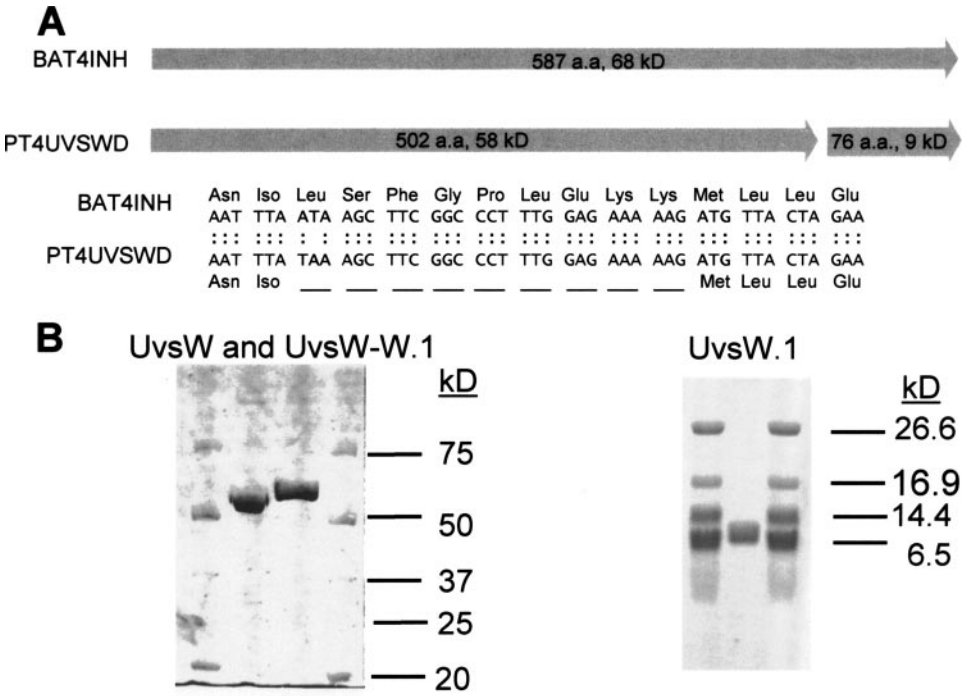

FIGURE 2. **Sequence discrepancy in the UvsW operon and purification of UvsW, UvsW.1, and UvsW-W.1 fusion.** *A*, the predicted open reading frames for two UvsW sequence depositions. A single T/A discrepancy results in either a 68-kDa polypeptide or 58- and 8-kDa polypeptides. Based on our sequencing and expression results, PT4UVSWD was deemed correct. *B*, SDS-PAGE gels demonstrating the purity of 58-kDa UvsW and the 68-kDa UvsW-W.1 engineered fusion protein (*left gel*) and 9-kDa UvsW.1 (*right gel*). Proteins were purified as described under "Materials and Methods." *a.a.*, amino acids.

of 295 nm was used specifically to excite the tryptophan residues of UvsW. Donor (UvsW) quenching and acceptor (UvsW.1) sensitization due to fluorescence resonance energy transfer was observed over a wavelength range between 305 and 580 nm. After the addition of UvsW.1 to the solution containing UvsW, the system was allowed to come to equilibrium for a period of 20 min. A blank spectrum containing only replication buffer was subtracted from all spectra. Identical experimental conditions were employed for experiments using direct excitation of UvsW.1-CPM at a wavelength of 385 nm.

Unwinding of R- and D-loop Plasmid-based Substrates—The R-loop unwinding reactions were performed in the standard replication buffer with 10 nM R-loop, 5 mM ATP, and 200 nM UvsW, UvsW/W.1, or UvsW-W.1 proteins in a total volume of 45 μl. After 30 s, an aliquot was removed from the reaction and quenched in 1 μg/μl proteinase K, 20 mM EDTA, 0.2% SDS, and loading buffer (25% Ficoll, 5 μg/ml xylene cyanol FF, and 4 μg/ml orange G). Reaction products were analyzed using 1% agarose gels run in 0.5× Tris borate EDTA buffer at 40 V for 16 h at room temperature. After electrophoresis, the agarose gel was dried on DE81 paper and exposed to a phosphorimaging plate overnight and analyzed using phosphorimaging.

The D-loop unwinding reactions were carried out by adding UvsW, UvsW/W.1, or UvsW-W.1 (200 nM) to an ongoing RecA-catalyzed strand invasion reaction (see above). After the addition of helicase, the reactions were quenched after 30 s and treated in an identical manner as the R-loop reactions.

Unwinding and ssDNA Annealing Assays Using Oligonucleotide-based Substrates—Unwinding and annealing assays were performed under identical conditions. Reactions were carried out at 37 °C in replication buffer containing 5 mM ATP (where indicated) with DNA and protein concentrations given in the figure legends. Where indicated, UvsW.1 or gp32 were added to yield final concentrations of 200 nM and 1 μM, respectively. Reactions were quenched at various time points with 1 μg/μl proteinase K, 20 mM EDTA, 0.2% SDS, and loading buffer (50% glycerol, 1 μg/ml bromphenol blue, 1 μg/ml xylene cyanol FF). Reaction products were analyzed using a 10% polyacrylamide gel run in 1× Tris borate EDTA buffer at 25 mA for 3 h at room temperature. Gels were exposed to a phosphorimaging plate overnight and analyzed using phosphorimaging.

RESULTS

Cloning, Expression, and Purification of UvsW Helicase—It has been noted that there is a discrepancy in the sequence of UvsW gene (Ref. 16, Fig. 2*A*). The UvsW operon found in the Entrez sequence data base (BAT4INH) encodes for a single 68-kDa protein, whereas the operon found in the T4 genome data base (PT4UVSWD, Tulane University) encodes for two polypeptides annotated as UvsW (58 kDa) and UvsW.1 (8.8 kDa). To determine which of these sequence entries is correct, we PCR-amplified T4 genomic DNA and sequenced the entire operon. Our results are consistent with the Tulane data base, indicating that there are indeed two separate polypeptides encoded within the UvsW operon. Due the reported poor solubility of UvsW, we cloned the open reading frame for UvsW (58 kDa) into several different expression vectors (pet28 with no tag, pet28 with an N-terminal hexahistidine tag, pet28 with a C-terminal hexahistidine tag, and pTYB3 with a C-terminal chitin binding and intein domains). Of these vectors, pet28 with an N-terminal hexahistidine tag provided soluble protein that could be easily purified. No soluble protein was recovered using the other constructs that were tested. The N-terminal His-tagged protein eluted from the nickel column containing a small amount of DNA contamination (as evidenced by an absorbance at 260 nM), which is removed by the additional phosphocellulose chromatography step (Fig. 2*B*).

Cloning, Expression, and Purification of UvsW.1 and UvsW/W.1 Fusion Proteins—To determine whether the UvsW.1 gene is efficiently translated within *E. coli*, we cloned the entire operon into the pTYB3 vector. This vector supplies a C-terminal chitin binding and intein domain (CBD/intein), which allows for rapid purification of full-length protein without additional amino acids (22). Because the CBD/intein is fused to the 3′-end of the operon, protein will be captured by the chitin column if UvsW.1 is expressed from the transcript. SDS-PAGE

Downloaded from http://www.jbc.org/ at IOWA STATE UNIV on March 28, 2016

analysis indicates that the UvsW.1-CBD/intein fusion is highly expressed within *E. coli* (data not shown), and we were able to capture this protein with the chitin column and efficiently elute UvsW.1 at a high level of purity (Fig. 2*B*).

To investigate the properties of a fusion between UvsW and UvsW.1 (referred to as UvsW-W.1; UvsW/W.1 indicates a mixture of two separate proteins), we removed the stop codon in the UvsW operon in the pTYB3 vector. This resulted in the overexpression of a soluble 68-kDa protein fused to the CBD/intein domain, which is captured by the chitin column and elutes normally with overnight incubation with β-mercaptoethanol (Fig. 2*B*). Apparently, fusion of the UvsW.1 protein to the C terminus of UvsW overcomes the solubility problems associated with expression of UvsW in isolation. Similar to UvsW, the UvsW-W.1 fusion protein also contained DNA contamination that is removed through phosphocellulose chromatography.

Fluorescence Experiments—The proximity of the open reading frame for UvsW.1 to the open reading frame of UvsW suggested that these two proteins might form a complex. To test for an interaction between UvsW and UvsW.1, we labeled UvsW.1 on its only cysteine residue (Cys^{24}) with CPM dye. UvsW.1 contains no tryptophan residues, allowing the eight tryptophan residues of UvsW to act as fluorescent donors to the CPM acceptor on UvsW.1. As shown in Fig. 3*A*, there is strong fluorescence resonance energy transfer between UvsW and UvsW.1 indicated by the decrease in the fluorescence of UvsW (λ_{max} of 340 nM) and a large increase in the fluorescence of UvsW.1-CPM (λ_{max} of 465 nM). The slight blue shift in the λmax of UvsW.1-CPM indicates that the change in fluorescence properties of the CPM dye is due to a change in environment in addition to *bona fide* fluorescence resonance energy transfer from UvsW. Indeed, when directly exciting the CPM dye (excitation = 360 nM), an increase in the fluorescence of UvsW.1-CPM was observed upon the addition of UvsW (Fig. 3*B*).

Nucleotide Hydrolysis Activity—Several nucleotide triphosphates were tested using ssM13 as a substrate. Due to multiple regions of highly stable secondary structure, ssM13 contains both ssDNA and dsDNA regions. Using this substrate, UvsW is able to hydrolyze both ATP and GTP, with a slight preference for ATP (supplemental Fig. 1*A*). The K_mATP is 170 ± 40 μM with a turnover number (k_{cat}) of 50.1 ± 3.4 s^{-1} (supplemental Fig. 1*B*) We also examined the ATPase activity of UvsW in the presence of short oligonucleotides. UvsW is both a ssDNA- and a dsDNA-dependent ATPase, hydrolyzing ATP in the presence of a wide variety of DNA structures, including blunt dsDNA and ssDNA (supplemental Fig. 1*C*).

Unwinding Assays—To confirm that our preparation of UvsW unwinds origin bound R-loops (11), we used a plasmid based system containing a 0.6-kilobase fragment corresponding to the oriF region of the T4 genome. Transcription from the plasmid encoded T7 promoter results in the formation of a stably bound transcript resistant to RNaseA but susceptible to RNase H or thermal denaturation (data not shown). Treatment of the R-loop-containing plasmid with UvsW, UvsW/W.1, or UvsW-W.1 in the presence of ATP leads to the dissociation of

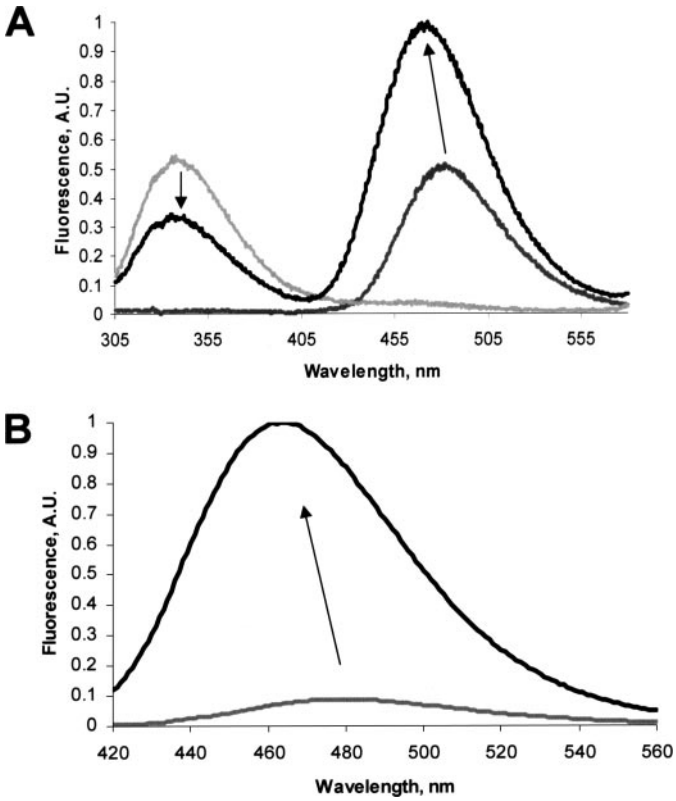

FIGURE 3. **Interaction between UvsW and UvsW.1.** *A*, fluorescence resonance energy transfer between the tryptophan residues of UvsW (donor) and the CPM dye attached to a single cysteine residue of UvsW.1 (acceptor) using an excitation wavelength of 295 nM. The fluorescent spectrum of UvsW, UvsW.1-CPM, and UvsW/W.1-CPM is shown in *light gray*, *dark gray*, and *black*, respectively. The *arrows* represent the change in fluorescence of UvsW and UvsW.1 upon the addition of the other protein. *B*, fluorescence of UvsW.1-CPM in the presence and absence of UvsW using direct excitation of the CPM dye at an excitation wavelength of 385 nM. The fluorescent spectrum of UvsW.1-CPM and UvsW/W.1-CPM is shown in *light gray* and *black*, respectively. *A.U.*, arbitrary units.

the R-loop (Fig. 4*A*). This reaction is extremely efficient, with complete dissociation of the R-loop in 30 s.

We also tested the ability of UvsW helicase to unwind a D-loop using an oligonucleotide/plasmid-based substrate (Fig. 4*B*). The supercoiled plasmid is identical to that used for the R-loop experiment, but the primer strand is an 80-base DNA oligonucleotide rather than a RNA polymerase-synthesized mRNA transcript. UvsW, UvsW/W.1, or UvsW-W.1 proteins were added to an ongoing reaction (2 min before the addition) containing plasmid, oligonucleotide, and RecA. Carried out in this manner, the RecA-catalyzed strand invasion reaction is occurring simultaneously with the unwinding activity of UvsW. As shown, all three proteins catalyze similar amounts of D-loop dissociation during the 30 s unwinding reaction. A time course indicates an ATP-dependent loss of D-loops with an observed rate of ~1.5 min^{-1} under our conditions (Fig. 4*C*).

We tested several oligonucleotide-based DNA structures as substrates for the unwinding activity of UvsW. UvsW, UvsW/W.1, and UvsW-W.1 were tested against each substrate both in the absence (data not shown) and presence (Fig. 5) of T4 single-strand DNA-binding protein (gp32). In the absence of gp32 under these assay conditions, there is a low level of helicase activity (less than 5% DNA unwinding) in the order of UvsW/

Downloaded from http://www.jbc.org/ at IOWA STATE UNIV on March 28, 2016

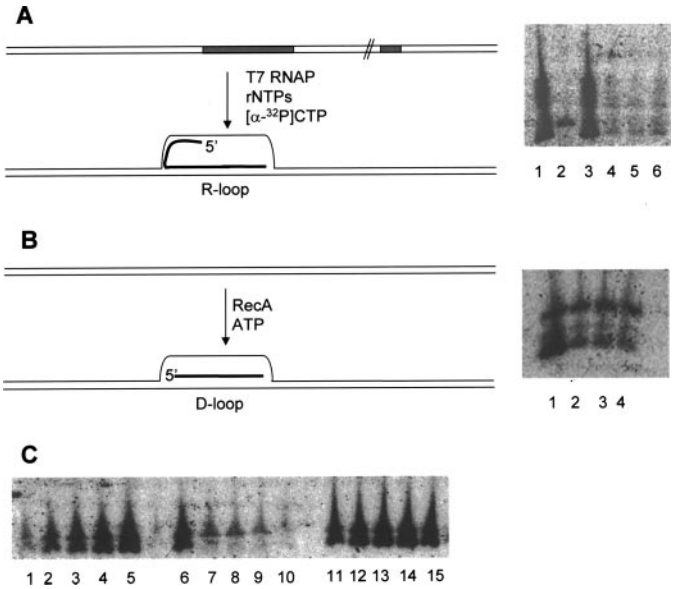

FIGURE 4. **UvsW unwinding of R- and D-loop.** *A*, a schematic of the construction of the plasmid based R-loop substrate. T7 RNA polymerase (*RNAP*) was used to transcribe a radiolabeled mRNA transcript that remains stably bound within the T4 origin cloned into a pGEM vector. Shown next to the schematic is the R-loop substrate untreated or treated with 95 °C heat, UvsW, UvsW + ATP, UvsW/W.1 + ATP, or UvsW-W.1 + ATP in *lanes 1–6*, respectively. *B*, a schematic of the construction of the plasmid based D-loop substrate. In the presence of ATP RecA protein catalyzes the strand invasion of a 5′-^{32}P-labeled 80-bp oligonucleotide into the supercoiled pGEM vector. Shown *next to the schematic* is the D-loop substrate untreated or treated with UvsW + ATP, UvsW/W.1 + ATP, or UvsW-W.1 + ATP in *lanes 1–4*, respectively. *C*, time courses of UvsW-catalyzed D-loop formation and unwinding. *Lanes 1–5* show the time-dependent RecA-catalyzed D-loop formation without UvsW addition with time points of 0.5, 1, 2, 3, and 4 min, respectively. *Lanes 6–10* are from a reaction where UvsW was added to an ongoing RecA reaction at 1.45 min in the presence of ATP with times points of 2, 2.25, 2.5, 3, and 4 min, respectively. *Lanes 11–15* are from a reaction where UvsW was added to an on-going RecA reaction at 1.45 min in the presence of ATPγS with time points of 2, 2.25, 2.5, 3, and 4 min, respectively.

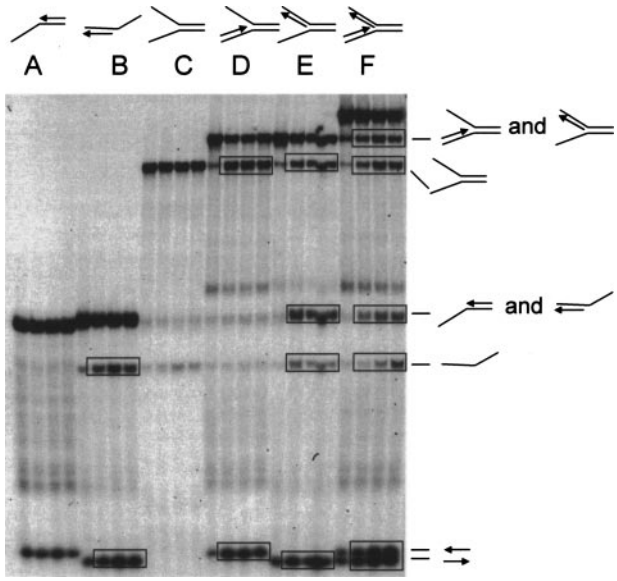

FIGURE 5. **Substrate specificity of UvsW unwinding activity.** All reactions contain 5 mM ATP and were performed for 2 min at 37 °C. Substrate and protein concentrations were 2 and 200 nM, respectively. The structures of substrates *A–F* can be found *above* the native PAGE gel. Unwinding reactions are performed in the presence of gp32 ssDNA-binding protein. For each substrate, the four reactions represent (from *left* to *right*) the addition of no UvsW, UvsW, UvsW/W.1, or UvsW-W.1. The unwinding products are highlighted by *black boxes* and were chosen based on an increase in signal over the mock reaction performed without the addition of UvsW protein. The DNA structures of the unwinding products are shown on the *right*.

W.1 = UvsW-W.1 > UvsW. Substrate specificity of DNA unwinding appears to be unaltered by the presence or absence of gp32. UvsW is capable of unwinding a simple duplex containing a 3′ ssDNA (substrate B) overhang but not a 5′ ssDNA overhang (substrate A). This type of substrate preference is consistent with the prediction that UvsW translocates on DNA in a 3′ to 5′ direction. Several branched DNA structures resembling stalled replication forks are also substrates for the unwinding activity of UvsW. The short arm(s) of substrates D, E, and F are all unwound from the DNA fork structures. Time courses of unwinding reactions using substrates D, E, and F reveal that only a fraction of the available substrate is unwound (Fig. 6). At the DNA concentrations used, spontaneous annealing cannot be the cause of this phenomenon. Likewise, trapping of the protein by the unwound strand can be ruled out because the ratio of protein to DNA is much greater than unity.

Annealing Activity of UvsW—As noted above, when short oligonucleotides are used as substrates, UvsW does not completely unwind all of the available DNA substrate. We also noticed that in some unwinding time courses, a burst of ssDNA product was seen, which was then followed by a decrease in the observed product (data not shown). For these reasons, we assayed UvsW for annealing activity. As seen in Fig. 7*A*, UvsW contains a potent ssDNA annealing activity. The reactions were performed in identical conditions as the unwinding assays using a substrate concentration of 0.2 nM to eliminate possible spontaneous annealing of the ssDNA strands. Under our conditions, the half-life for spontaneous annealing is ~105 min (0.0095 min^{-1}). The addition of ATP to the reaction increases the annealing activity; however, ATPγS strongly inhibits the reaction, indicating ATP binding alone is not sufficient for the activation in annealing rate. Also, the addition of T4 ssDNA-binding protein (gp32) in the presence of ATP significantly reduces but does not completely inhibit the UvsW-catalyzed annealing. In the presence of ATP, preincubation of UvsW with an equimolar concentration of UvsW.1 cause a reduction in annealing rate (Fig. 7*B*). The UvsW-W.1 fusion protein has a similar annealing rate as the UvsW/W.1 mixture at early time points but appears to reach a steady state before the ssDNA is fully annealed. A likely explanation for this is that an equilibrium exists between free UvsW and UvsW in complex with UvsW.1. This would allow a higher degree of annealing than in the situation where the two proteins are fused and dissociation of the complex is not possible.

The oligonucleotide-based substrates were tested for UvsW-catalyzed annealing activity (Fig. 8). These reactions reveal differences in annealing rates generally correlating with the polarity and complexity of the DNA substrates. A comparison of substrates A and B indicates a strong dependence on the polarity of the ssDNA strands. Substrate A is efficiently annealed by UvsW, whereas the annealing rate of substrate B is only slightly greater than the rate of spontaneous annealing. The ssDNA strands of substrate C and D are annealed at a rate intermediate to substrates A and B, whereas substrates E and F are annealed

Downloaded from http://www.jbc.org/ at IOWA STATE UNIV on March 28, 2016

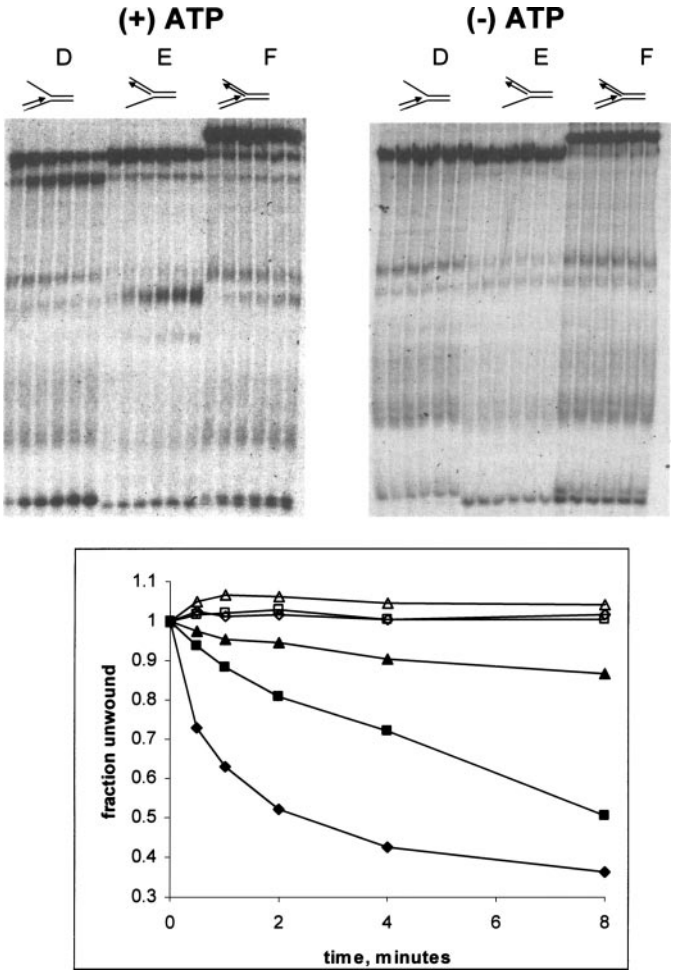

FIGURE 6. **Time course of UvsW unwinding on model-stalled replication forks in the presence of gp32.** All reactions were carried out at 37 °C with ATP (where indicated), substrate, and UvsW concentrations of 5 mM, 2 nM, and 200 nM, respectively. The structures of substrates *D–F* can be found *above* the native PAGE gel. Quantification of the unwinding products is shown as a plot of fraction substrate unwound *versus* time. Substrates *D–F* are represented by *diamonds*, *squares*, and *triangles*. *Open* and *closed symbols* represent reactions carried out in the absence and presence of ATP, respectively. Fraction substrate unwound is calculated by dividing the amount of radioactivity in the substrate band by the total amount of radioactivity contained in the bands for the substrate and all the unwound products.

at a reduced rate. All substrates are annealed by UvsW at rates above that of spontaneous annealing.

The substrate specificity, unwinding activity, and annealing activity of the N-terminal His-tagged UvsW protein (in the presence of an equimolar amount of UvsW.1) are very similar to the non-tagged UvsW-W.1 fusion protein. This strongly suggests that the properties of UvsW are not altered by the introduction of the hexahistidine tag. This result is expected since the N terminus of UvsW is not near the predicted ATP or DNA binding sites (see Fig. 1).

DISCUSSION

Helicases are versatile enzymes that are involved in virtually every process related to DNA and RNA metabolism. As expected, because of the wide variety of substrates that helicases are required to act upon, there are a multitude of helicases found in all living organisms. There are 11 known helicases in *E. coli* and at least 24 in humans. In contrast, there are only three helicases encoded for by T4 phage, an organism that supplies all the necessary proteins for the replication of its genome. Additionally, T4 phage is capable of undergoing genomic recombination, DNA repair, and genomic maintenance (1). T4 phage has been an outstanding model for the study of DNA replication (23, 24), and because of its simplified repertoire of DNA recombination and repair proteins (25), we expect it will become an excellent model system for the study of these processes as well. Several T4 proteins implicated in DNA recombination and repair are not well characterized. Among these is UvsW, which is part of the UvsWXY system of genes that, when mutated, confers a sensitivity to DNA damaging agents such as UV light or hydroxyurea (12–14). *In vivo* experiments have shown that UvsW is involved in recombination-dependent DNA repair, and *in vitro* experiments have demonstrated that it is capable of dissociating R-loops and a branched DNA substrate (9, 11). However, partially due to the difficulty in expression and purification of soluble protein (16), a more complete biochemical analysis of UvsW has been lacking.

UvsW has been identified as a functional homolog of RecG based on its ability to complement some of the defects of a RecG$^-$ *E. coli* mutant (9). However, the substrate specificity shown in Fig. 4 differs from that of RecG (*i.e.* RecG is incapable of unwinding non-branched DNA structures). Moreover, aside from the RecA-like helicase domain found in all type 2 helicases, the structure of the N-terminal fragment of UvsW significantly differs from that of RecG. This structural difference led White and co-workers (16) to conclude that RecG and UvsW must use different mechanisms for substrate recognition, consistent with the differing substrate specificities seen here. From our analysis, it appears that UvsW is more flexible in terms of its substrate specificity when compared with RecG. UvsW is capable of unwinding branched DNA structures similar to RecG, but it can also unwind simple DNA duplexes with overhanging 3′ tails. UvsW can also dissociate the invading strand of a D-loop. All these reactions require ATP and its subsequent hydrolysis. Based on this substrate specificity, UvsW is functionally more similar to the RecQ family of helicases (26). RecQ DNA helicases, like RecG, are also members of the SF2 family and have been implicated in DNA replication, recombination, and repair (27).

Another similarity between UvsW and some members of the RecQ family is the ability to catalyze the annealing of complementary ssDNA strands. Human RecQ helicases such as Blooms, Werner, RecQ5β, RecQ1, and RecQ4 all possess ssDNA annealing activity (28–32). To our knowledge, with the exception of this report, no ssDNA annealing activity has been found in any helicase outside the RecQ family. The annealing activity of both UvsW and RecQ helicases is reduced in the presence of single-stranded binding protein. However, even at a saturating concentration of gp32, UvsW anneals ssDNA at least ~5 times faster than the rate of spontaneous annealing. It has been reported that gp32 itself contains ssDNA annealing activity (33, 34). This was not observed in our studies, possibly due to the large difference in ssDNA concentration (we used 20-fold less ssDNA). In addition to the differing responses to ssDNA-binding protein, other factors such as the presence of nucleotides affect the annealing rates of UvsW and human RecQ heli-

Downloaded from http://www.jbc.org/ at IOWA STATE UNIV on March 28, 2016

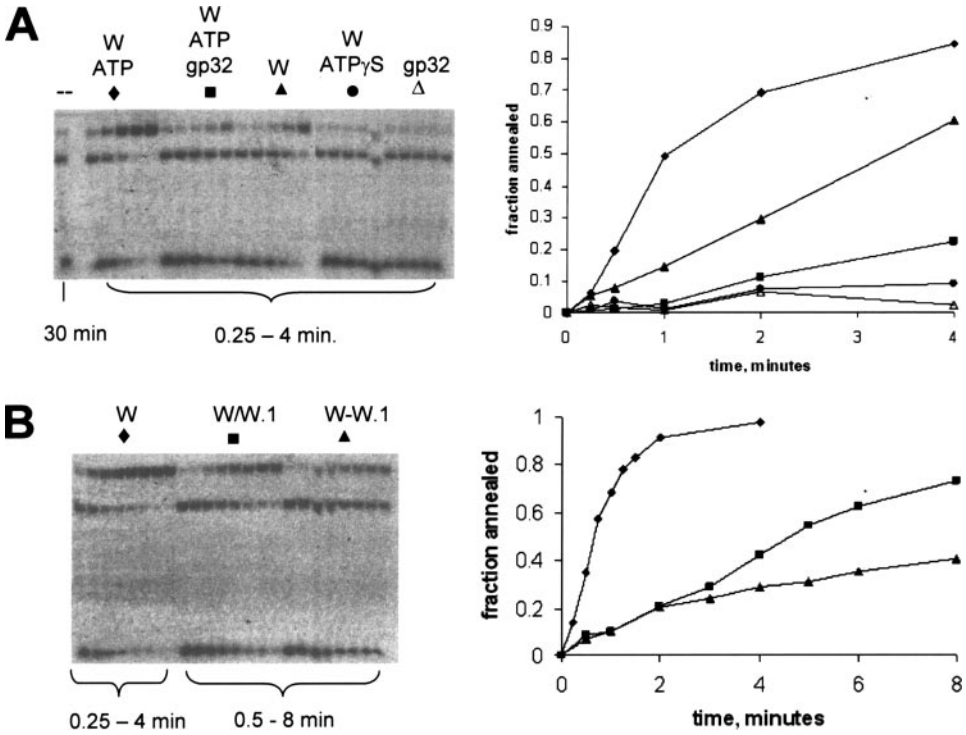

FIGURE 7. **Annealing activity of UvsW under various conditions.** All reactions contain 5 mM ATP and were carried out at 37 °C with substrate and protein concentrations of 0.2 and 200 nM, respectively. The ssDNA strands used are from substrate A found in Table 1. *A*, time courses of UvsW-catalyzed ssDNA annealing. The conditions of the reactions are listed *above* each time course. Quantification of the annealing reactions is shown as a plot of fraction substrate annealed *versus* time. The conditions represented by each *symbol* are shown *above* the gel. Fraction substrate annealed is calculated by dividing the amount of radioactivity in the product band by the total amount of radioactivity contained in the bands for the product and the ssDNA substrates. *B*, time courses of ssDNA annealing in the presence of ATP catalyzed by UvsW, UvsW/W.1, and UvsW-W.1 proteins. Quantification is performed the same as in *A*. The conditions represented by each symbol are shown *above* the gel.

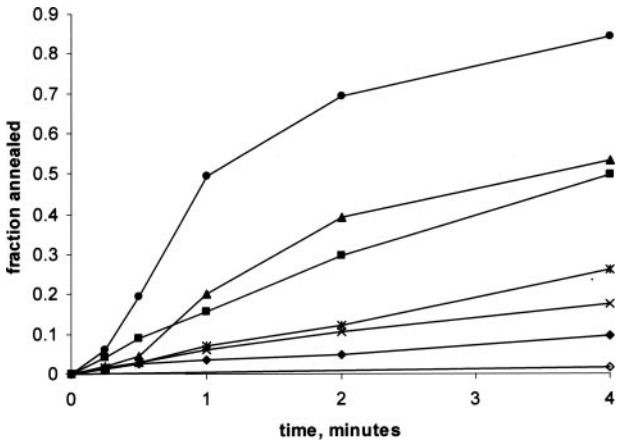

FIGURE 8. **Substrate specificity of UvsW annealing activity.** All reactions contain 5 mM ATP and were performed at 37 °C. Substrate and protein concentrations were 0.2 and 200 nM, respectively. Quantification of the annealing reactions is shown as a plot of fraction substrate annealed *versus* time. Fraction substrate annealed is calculated by dividing the amount of radioactivity in the product band by the total amount of radioactivity contained in the bands for the product and the ssDNA substrates. The ssDNA strands used are from substrates A (*circles*), B (*diamonds*), C (*squares*), D (*triangles*), E (*asterisks*), and F (*cross-hatches*). The spontaneous annealing rate of substrate A is shown by *open triangles*. The structures of substrates A–F can be found in Table 1.

cases differently. For example, the annealing activity of UvsW is activated by ATP and completely inhibited by ATPγS, whereas RecQ1 and Blooms helicase are partially inhibited by both these nucleotides (28, 31). However, unlike the helicase activity, strand annealing by UvsW does not have an absolute requirement for ATP, although the presumed hydrolysis of ATP accelerates the processes. Similarly to UvsW, RecQ5B helicase is only inhibited by ATPγS and not ATP. A possible mechanistic explanation for these differences is given below.

One postulated annealing mechanism, based upon the proposed mechanism for human Mre11 protein, involves the dimerization of ssDNA-bound proteins to bring the complementary strand into close proximity (35, 30). This mechanism may not apply to UvsW or other members of RecQ family that promote ssDNA annealing, as only RecQ1 has been shown to be a dimer in solution. Based on the crystal structure of the N-terminal domains of UvsW, it has been suggested that there are at least two regions that interact with DNA substrate. The two RecA-like domains, which contain all seven of the S2 helicase motifs and are thought to be the domains responsible for ATP-coupled translocation undoubtedly interact with the DNA substrate. Also, the unique N-terminal domain of UvsW, which is structurally similar to the transcription factor MotCF is also expected to bind to DNA (17). Based on these multiple DNA binding domains, we suggest an ssDNA annealing mechanism similar to that proposed for the RecQ1 dimer but only requires an UvsW monomer (Fig. 9). In this model the RecA-like domains bind one strand of ssDNA, whereas the MotCF domain binds the other. The proximity of these domains facilitates the annealing of the complementary DNA strands.

This mechanism also accounts for the ATP activation effect. In half of the binding events, the UvsW monomer will bind non-complementary ssDNA strands (*i.e.* ssDNA strand of identical sequence). This would represent a dead-end complex and would essentially sequester the DNA substrate and prevent its annealing until the at least one of the ssDNA strands dissociates from the enzyme complex. ATP hydrolysis would allow UvsW to actively translocate off the ssDNA strand bound to the helicase domain, thereby allowing another ssDNA to be captured. This would effectively serve to increase the ssDNA annealing rate. This annealing mechanism also accounts for the inhibition by ATPγS. ATPγS may stabilize the unproductive ssDNA·UvsW·ssDNA complex, preventing escape by inhibiting both translocation and simple dissociation. Translocation may also be required when UvsW binds the correct ssDNA strands. In the event that the bound strands are not properly

Downloaded from http://www.jbc.org/ at IOWA STATE UNIV on March 28, 2016

aligned for annealing, translocation on the ssDNA strand bound to the helicase domain may be necessary for alignment. Based on this mechanism, differences between helicases regarding nucleotide requirement and inhibition stem from different stabilities of the helicase-ssDNA unproductive complexes.

The mechanism of partial inhibition of UvsW catalyzed annealing by UvsW.1 is unclear. The fusion of UvsW.1 to the C terminus of UvsW results in a protein with similar properties as UvsW in the presence of UvsW.1. Because of the relatively short linker between UvsW and UvsW.1 (9 amino acids), the binding locus for UvsW.1 must be near the C terminus of UvsW. Unfortunately, the C-terminal domain of UvsW is not present in the available crystal structure. UvsW.1 is a highly acidic protein (pI 4.24), making it a likely binding partner for one of the highly basic patches on the surface of UvsW that are predicted to interact with the DNA substrate (16). It is possible that the UvsW.1 prevents the binding of one of the ssDNA strands by a simple competitive mechanism. Assuming UvsW.1 can only block a single DNA binding site, a DNA substrate suitable for unwinding can still interact with the available DNA binding site on UvsW (most likely the helicase domains). This initial binding event would greatly increase the local concentration of DNA near the second binding site and would effectively displace UvsW.1. This increase in local concentration would only occur with substrates meant to be unwound, since in strand-annealing reactions, the binding of one ssDNA strand does not affect the local concentration of the other.

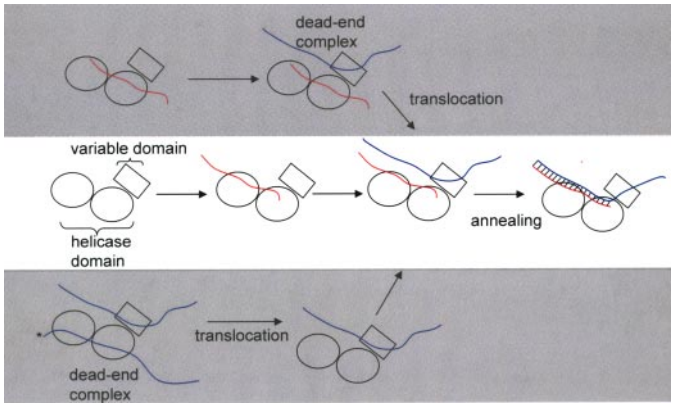

FIGURE 9. **Possible annealing mechanism for UvsW.** The ATP independent annealing pathway is shown in *light gray*. The binding of two ssDNA strands by two separate domains of the protein brings the strands in close proximity. The annealing reaction occurs spontaneously. The ATP-dependent pathways are shaded in *dark gray*. When the ssDNA strand bound to the helicase domain is either not well aligned or not complementary to the ssDNA strand bound to the variable domain, ATP-driven translocation is required for alignment or dissociation, respectively. Further details can be found under "Discussion."

The attenuation of the annealing activity of UvsW by UvsW.1 suggests that other helicases with ssDNA annealing activity may be modulated by protein-protein interactions. Human helicases such as Blooms and Werner syndrome helicases have a multitude of different binding partners (a comprehensive list can be found in Ref. 36). Several of these binding partners increase the unwinding activity of the helicase. It is possible that some of these interactions actually serve to decrease the annealing activity of the helicase making unwinding more favorable.

The presence of two distinct enzymatic activities within the same protein may provide some information on the function the UvsW *in vivo*. Several of the recombination-dependent replication pathways that are postulated to be involved in replication fork repair involve both DNA unwinding and ssDNA annealing (Fig. 10). One of the more attractive DNA repair models involves fork regression (Fig. 10*A*), which requires the replication fork becomes uncoupled at the site of a lesion in the leading strand template. The uncoupling allows the primosome and lagging strand polymerase to synthesize an Okazaki fragment beyond the point of the DNA lesion. After uncoupling and disassembly of the replisome, the fork is regressed to allow the pairing of the nascent leading and lagging strands. Because the lagging strand has been synthesized beyond the DNA lesion, it becomes a template for leading strand extension. Finally, the fork is returned to its original configuration through a branch migration reaction, and replication restarts. UvsW is well suited for several steps of this pathway. The initial fork regression may occur via UvsW-catalyzed unwinding of the newly synthesized leading and lagging strands (as seen in Fig. 5) followed by their annealing, which also may be carried out by UvsW. UvsW could also be responsible for the resetting of the replication fork, as

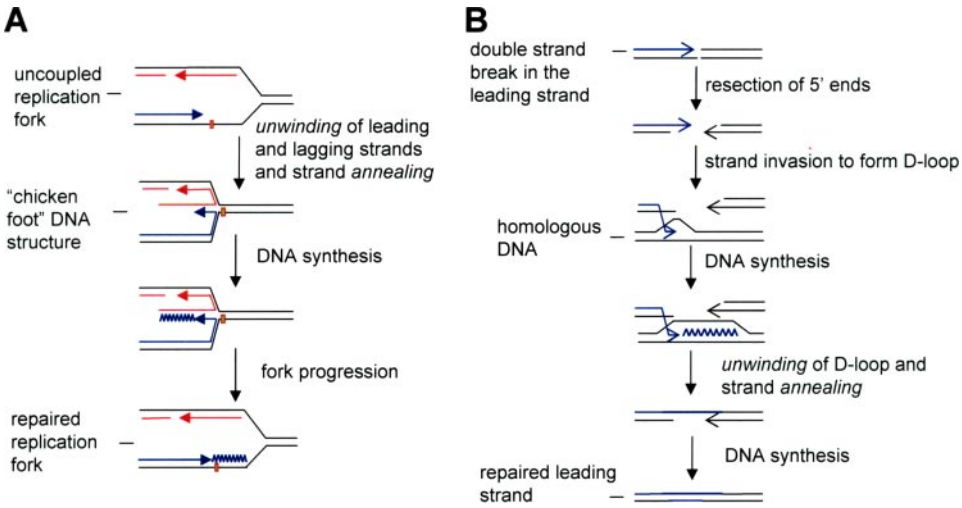

FIGURE 10. **DNA repair pathways requiring both unwinding and annealing activities.** *A*, leading strand lesion bypass. The uncoupling of the replisome at the site of a leading strand lesion creates a fork structure that may be unwound by a helicase. The annealing of the nascent leading and lagging strands results a "chicken-foot" DNA structure, allowing the leading strand to be copied using the lagging strand as a template. Fork progression resets the replication fork, and the leading strand has bypassed the lesion. *B*, the synthesis-dependent strand-annealing pathway. A nick in the DNA template leads to a double strands break. After resection of the 5′ ends, the ssDNA invades a homologous duplex DNA template forming a D-loop. The invading strand is extended by polymerase until it dissociates and anneals with its original DNA duplex. A second round of DNA synthesis and ligation completes the repair pathway.

Downloaded from http://www.jbc.org/ at IOWA STATE UNIV on March 28, 2016

it is capable of performing branch migration of four-way branched Holliday junction-like DNA substrates.[4]

The synthesis-dependent strand annealing (SDSA) pathway also requires both unwinding and annealing activities (Fig. 10*B*). SDSA is thought to be the most common mechanism for the processing of double-strand breaks during mitotic replication in eukaryotic organisms (37). In this model, the resection of the duplex DNA ends in the 5′ to 3′ direction by T4 gp46/47 results in two single-stranded 3′ ends. The ssDNA is now a substrate for UvsX/Y-catalyzed recombination with homologous duplex DNA. The invading strands of the D-loop are extended until the polymerases reach a barrier caused by the UvsX filament on the opposing end of the D-loop. After DNA synthesis, the invading strand must dissociate from its template, possibly through the action of a helicase. The resulting ssDNA strands then anneal with each other thus repairing the DNA break. UvsW is a strong candidate for mediating these later two events in the SDSA pathway.

The ability of UvsW to unwind recombination intermediates such as a D-loop would seems at odds with its proposed role in double-strand break repair and other DNA repair pathways. However, this appears to be a property of several DNA repair helicases, most notably Srs2 helicase from *Saccharomyces cerevisiae* (38). Srs2 is known as negative regulator of homologous recombination and has been shown to disassembly Rad51 nucleoprotein filaments (39). However, Srs2 is also required for efficient recombination-dependent double-strand break repair (40). Specifically, Srs2 facilitates the SDSA repair pathway described above, although the mechanism is unknown. It has been suggested that Srs2 may prevent a double-strand invasion event by removal of Rad51 from one of the ssDNA ends or may participate directly in SDSA by unwinding the D-loop, allowing the later steps of the pathway to proceed (37).

Clearly, the activities of UvsW are well suited for participating in many of the proposed DNA repair pathways, which is consistent with the *in vivo* effects of UvsW mutation. However, the precise role of UvsW in DNA repair will require the *in vitro* reconstitution of these pathways with other proteins thought to be involved in DNA replication and repair to determine how different enzymatic activities work together to manipulate the DNA structures.

REFERENCES

1. Miller, E. S., Kutter, E., Mosig, G., Arisaka, F., Kunisawa, T., and Ruger, W. (2003) *Microbiol. Mol. Biol. Rev.* **67,** 86–156
2. Young, M. C., Schultz, D. E., Ring, D., and von Hippel, P. H. (1994) *J. Mol. Biol.* **235,** 1447–1458
3. Schrock, R. D., and Alberts, B. (1996) *J. Biol. Chem.* **271,** 16678–16682
4. Raney, K. D., and Benkovic, S. J. (1995) *J. Biol. Chem.* **270,** 22236–22242
5. Eoff, R. L., and Raney, K. D. (2006) *Nat. Struct. Mol. Biol.* **3,** 242–249
6. Wakem, L. P., Zahradka, C. L., and Ebisuzaki, K. (1984) *Virology.* **137,** 338–346
7. Derr, L. K., and Kreuzer, K. N. (1990) *J. Mol. Biol.* **214,** 643–656
8. Woodworth, D. L., and Kreuzer, K. N. (1996) *Genetics* **143,** 1081–1090
9. Carles-Kinch, K., George, J. W., and Kreuzer, K. N. (1997) *EMBO J.* **16,** 4142–4151
10. Mosig, G., Colowick, N., Gruidl, M. E., Chang, A., and Harvey, A. J. (1995) *FEMS Microbiol. Rev.* **17,** 83–98
11. Dudas, K. C., and Kreuzer, K. N. (2001) *Mol. Cell. Biol.* **21,** 2706–2715
12. Derr, L. K., and Drake, J. W. (1990) *Mol. Gen. Genet.* **222,** 257–264
13. Conkling, M. A., and Drake, J. W. (1984) *Genetics* **107,** 505–523
14. Hamlett, N. V., and Berger, H. (1975) *Virology* **63,** 539–567
15. George, J. W., and Kreuzer, K. N. (1996) *Genetics* **143,** 1507–1520
16. Sickmier, E. A., Kreuzer, K. N., and White, S. W. (2004) *Structure* **12,** 583–592
17. Li, N., Sickmier, E. A., Zhang, R., Joachimiak, A., and White, S. W. (2002) *Mol. Microbiol.* **43,** 1079–1088
18. Velankar, S. S., Soultanas, P., Dillingham, M. S., Subramanya, H. S., and Wigley, D. B. (1999) *Cell.* **97,** 75–84
19. Singleton, M. R., Scaife, S., and Wigley, D. B. (2001) *Cell.* **107,** 79–89
20. Yang, J., Trakselis, M. A., Roccasecca, R. M., and Benkovic, S. J. (2003) *J. Biol. Chem.* **278,** 49828–49838
21. McIlwraith, M. J., Hall, D. R., Stasiak, A. Z., Stasiak, A., Wigley, D. B., and West, S. C. (2001) *Nucleic Acids Res.* **29,** 4509–4517
22. Chong, S., Montello, G. E., Zhang, A., Cantor, E. J., Liao, W., Xu, M.-Q., and Benner, J. (1998) *Nucleic Acids Res.*, **26,** 5109–5115
23. Benkovic, S. J., Valentine, A. M., and Salinas, F. (2001) *Annu. Rev. Biochem.* **70,** 181–208
24. Nossal, N. G. (1992) *FASEB J.* **6,** 871–878
25. Kreuzer, K. N. (2005) *Annu. Rev. Microbiol.* **59,** 43–67
26. Bennett, R. J., and Keck, J. L. (2004) *Crit. Rev. Biochem. Mol. Biol.* **39,** 79–97
27. Tuteja, N., and Tuteja, R. (2004) *Eur. J. Biochem.* **271,** 1849–1863
28. Cheok, C. F., Wu, L., Garcia, P. L., Janscak, P., and Hickson, I. D. (2005) *Nucleic Acids Res.* **33,** 3932–3941
29. Machwe, A., Lozada, E. M., Xiao, L., and Orren D. K. (2006) *BMC Mol. Biol.* **7,** 1
30. Liu, Y., Jiricny, J., West, S. C., and Janscak, P. (2004) *EMBO J.* **23,** 2882–2891
31. Sharma, S., Sommers, J. A., Choudhary, S., Faulkner, J. K., Cui, S., Andreoli, L., Muzzolini, L., Vindigni, A., and Brosh, R. M., Jr. (2005) *J. Biol. Chem.* **280,** 28072–28084
32. Macris, M. A., Krejci, L., Bussen, W., Shimamoto, A., and Sung, P. (2006) *DNA Repair* **5,** 172–180
33. Alberts, B. M., and Frey, L. (1970) *Nature* **227,** 1313–1318
34. Kantake, N., Madiraju, M. V., Sugiyama, T., and Kowalczykowski, S. C. (2002) *Proc. Natl. Acad. Sci. U. S. A.* **99,** 15327–15332
35. de Jager, M., Dronkert, M. L., Modesti, M., Beerens, C. E., Kanaar, R., and van Gent, D. C. (2001) *Nucleic Acids Res.* **29,** 1317–1325
36. Bachrati, C. Z., and Hickson, I. D. (2006) *Methods Enzymol.* **409,** 86–100
37. Pâques, F., and Haber, J. E. (1999) *Microbiol. Mol. Biol. Rev.* **63,** 349–404
38. Macris, M. A., and Sung, P. (2005) *Biochem. Soc. Trans.* **33,** 1447–1450
39. Veaute, X., Jeusset, J., Soustelle, C., Kowalczykowski, S. C., Le Cam, E., and Fabre, F. (2003) *Nature* **423,** 309–312
40. Ira, G., Malkova, A., Liberi, G., Foiani, M., and Haber, J. E. (2003) *Cell.* **115,** 401–411

[4] S. W. Nelson and S. J. Benkovic, unpublished results.

Downloaded from http://www.jbc.org/ at IOWA STATE UNIV on March 28, 2016

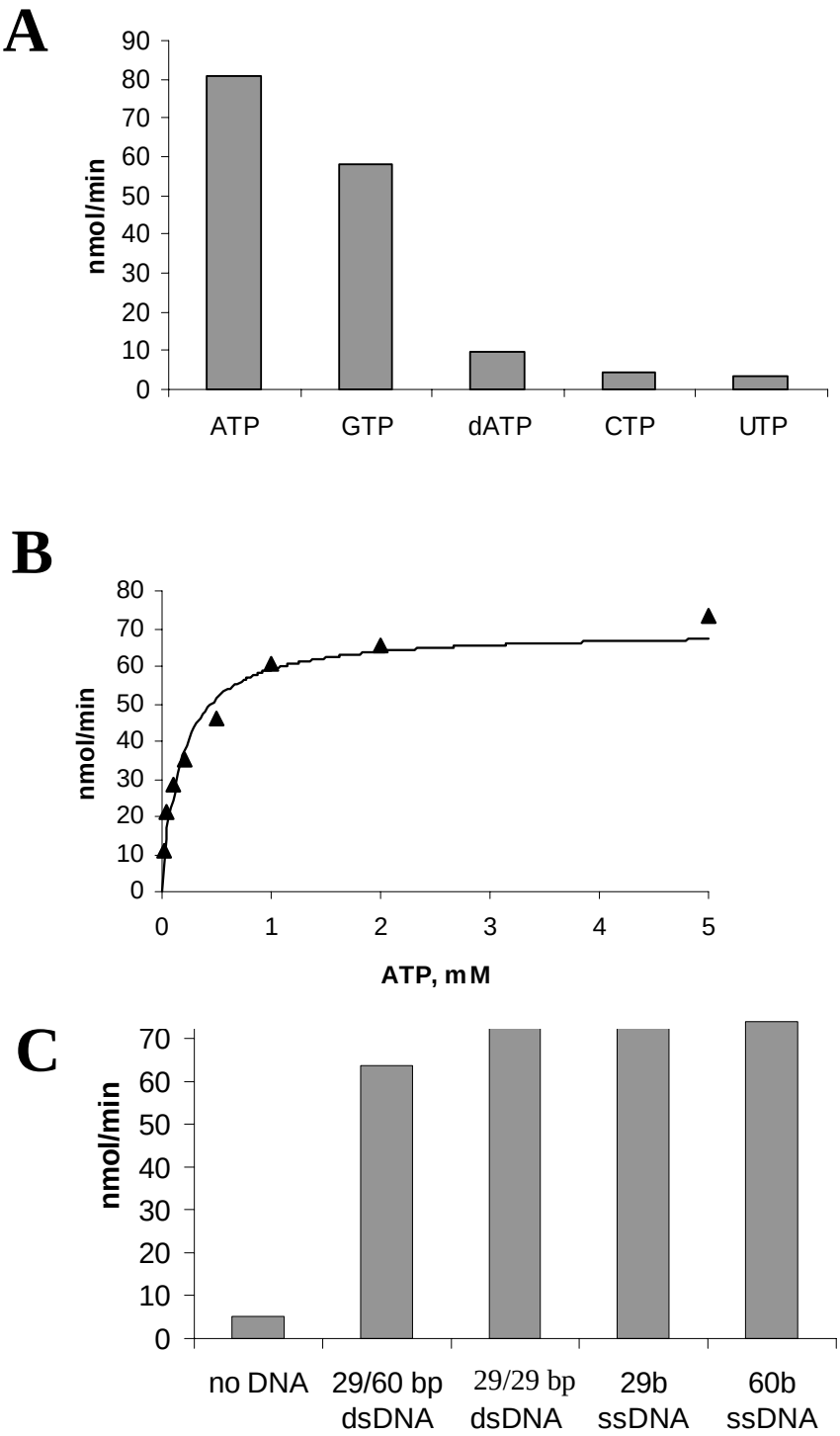

Supplementary Fig. 1. **Nucleotide hydrolysis activity of UvsW.** All reactions were performed as described in "Materials and Methods". The protein and DNA concentrations were 20 nM and 2 μM, respectively. *A.* The nucleotide dependence of UvsW-catalyzed nucleotide hydrolysis. The DNA substrate used in these reactions was ssM13. *B.* The data (triangles) was fit to the Michaelis-Menton equation (shown by solid line). The fitted parameters are $K_M = 170 \pm 40$ μM and *k*cat = 50.1 ± 3.4 sec^{-1}. *C.* The initial velocity of UvsW-catalyzed ATP hydrolysis using different DNA substrates.

The T4 Phage UvsW Protein Contains Both DNA Unwinding and Strand Annealing Activities

Scott W. Nelson and Stephen J. Benkovic

J. Biol. Chem. 2007, 282:407-416.
doi: 10.1074/jbc.M608153200 originally published online November 8, 2006

Access the most updated version of this article at doi: 10.1074/jbc.M608153200

Alerts:
- When this article is cited
- When a correction for this article is posted

Click here to choose from all of JBC's e-mail alerts

This article cites 39 references, 19 of which can be accessed free at
http://www.jbc.org/content/282/1/407.full.html#ref-list-1

Downloaded from http://www.jbc.org/ at IOWA STATE UNIV on March 28, 2016